Am J Cancer Res 2025;15(3):1291-1306
www.ajcr.us /ISSN:2156-6976/ajcr0162469

Original Article

Development and validation of a Nomogram to predict postoperative flap necrosis risk in breast cancer patients undergoing modified radical mastectomy

Yi Peng, Xin Zhang, Jianbin Wu, Hongmei Wang, Xiaoxi Huang

Department of Breast Surgery, Fujian Maternity and Child Health Hospital, Fuzhou 350001, Fujian, China

Received December 5, 2024; Accepted March 12, 2025; Epub March 15, 2025; Published March 30, 2025

Abstract: Background: Flap necrosis is a critical complication following modified radical mastectomy (MRM) for breast cancer (BC). It not only impairs wound healing but also delays postoperative treatment, adversely affecting patient survival rate and the overall quality of life. Thus, developing an accurate prediction model is crucial for early intervention and improving patient prognosis. Objective: To develop and validate a Nomogram model based on Logistic regression to assess the risk of postoperative flap necrosis in BC patients undergoing MRM. Methods: A retrospective study was conducted on 605 BC patients who underwent MRM. These patients were stratified into a training group (n=406) and a validation group (n=199) in a 33:67 ratio. Univariate and multivariate Logistic regression analyses were performed to identify risk factors for flap necrosis, and a Nomogram prediction model was subsequently constructed. The model's discriminatory power (assessed via the receiver operating characteristic [ROC] curve), calibration accuracy (evaluated by calibration curve), and clinical benefit (analyzed through decision curve analysis) were comprehensively evaluated. Moreover, essential performance metrics such as sensitivity, specificity, and accuracy were systematically recorded and analyzed. Results: Nine independent risk factors were identified, including age, body mass index (BMI), neutrophil count, hemoglobin level, drainage volume on the third postoperative day, axillary lymph node metastasis (ALNM), surgical duration, intraoperative bleeding volume, and drainage duration. The area under the curve (AUC) of the Nomogram model was 0.898 in the training group and 0.886 in the validation group, indicating good discriminatory capacity. Calibration curves demonstrated good agreement between predicted values and actual values, with P-values for goodness-of-fit of 0.1761 (training) and 0.0648 (validation), respectively. Decision curve analysis revealed significant clinical benefits, with maximum benefit rates of 76.84% (training) and 80.40% (validation), respectively. Conclusion: The Nomogram model developed in this study accurately predicts flap necrosis risk in BC patients post-MRM, offering significant clinical utility for risk management and improved patient outcomes.

Keywords: Breast cancer, flap necrosis, modified radical mastectomy, logistic regression, Nomogram

Introduction

Breast cancer (BC) ranks among the most prevalent malignant tumors afflicting women worldwide. It is characterized by the aberrant proliferation of breast epithelial cells, which can manifest as either localized or invasive growth patterns and may potentially metastasize distantly via the hematogenous or lymphatic systems [1, 2]. As per the 2020 Global Cancer Report, BC surpassed lung cancer as the most frequently diagnosed cancer globally, with 2.26 million new cases. In China, approximately 416,000 BC cases were reported among women, constituting 18.4% of the global total, with an incidence rate of 59.0 per 100,000 [3]. BC has now become the leading malignancy among Chinese women, exhibiting a progressively ascending incidence rate and a trend toward younger age at diagnosis [4].

The therapeutic regimens for BC involve a comprehensive array of modalities such as surgery, chemotherapy, radiotherapy, endocrine therapy, and targeted therapy. Among these, surgical treatment remains the cornerstone of disease management [5]. In China, modified radical mastectomy (MRM) is the most commonly employed surgical approach for BC [6]. While advancements in surgical techniques and adju-

https://doi.org/10.62347/DYFF7059

vant therapies have considerably enhanced patient survival rate, postoperative complications continue to adversely affect rehabilitation quality and long-term outcomes [7]. MRM involves the removal of the breast, adjacent thoracic wall tissues, and axillary lymph nodes while preserving the pectoral muscles, which covers extensive operative field and results in substantial trauma [8]. Nevertheless, the transection of numerous small blood vessels and lymphatic ducts during MRM creates a potential space between the skin flap and the thoracic wall, complicating postoperative wound healing. Common complications Common subcutaneous fluid accumulation, wound infection, hematoma, adipose tissue necrosis, and flap necrosis [9].

Flap necrosis is one of the gravest wound complications following MRM for BC, with reported incidence spanning from 10% to 61% [10, 11]. This condition arises from inadequate tissue blood perfusion. Flap necrosis not only prolongs postoperative wound healing but may also trigger infections, wound dehiscence, and other severe complications [12]. These circumstances result in extended hospital stays, increased medical expenses, and delays the seamless execution of comprehensive postoperative therapies. Research [13] has demonstrated that postponing adjuvant treatments (e.g., chemotherapy, radiotherapy) for over 12 weeks due to wound complications significantly worsens patient survival outcomes, including a reduced disease-free survival rate and an increased risk of recurrence. Additionally, postoperative wound complications negatively impact patient's psychological well-being, body image, and quality of life, exacerbating doctor-patient conflicts and treatment-related stress [14].

Prevention is the most effective approach to reduce the incidence of postoperative flap necrosis. Nevertheless, the development of flap necrosis is influenced by multiple factors, such as the patient's preoperative physical state, comorbidities, intraoperative procedures, and postoperative management. The interplay of these factors varies significantly among patients, making it challenging to predict the risk of flap necrosis based solely on clinical experience. Consequently, a mathematical model incorporating comprehensive multi-factorial analysis has become essential for identifying high-risk patients. In this study, we retrospectively analyzed wound complications occurring 90 days after MRM for BC. We systematically screened preoperative and intraoperative risk factors related to flap necrosis and developed a risk prediction model based on Logistic regression. This model provides a scientific tool for clinical risk assessment by quantifying individual patient risk profiles. Additionally, we created a Nomogram to visualize the model and conducted internal validation to evaluate its discriminatory power, calibration accuracy, and clinical utility.

Methods and data

Sample size calculation

With reference to the study by Hannah R Ray et al. [11], which reported a 44% incidence rate of flap necrosis following MRM for BC, the sample size for this study was calculated according to the requirements of Logistic regression analysis. A confidence level of 95% and an allowable error of 5% were set. Using the formula $N = Z^2 \times [P \times (1 - P)]/E^2$, the minimum sample size required for this study was determined to be 380 cases. To account for potential data censoring or missing data (approximately 10%) and to enhance statistical power while reducing sample bias, the final plan aimed to enroll at least 420 patients.

Research design

In this retrospective single-center study, data from patients (n=605) who underwent MRM for BC during May 2018 and May 2024 were collected from the breast surgery department of Fujian Maternity and Child Health Hospital. The study period was. This study was approved by the Ethics Committee of Fujian Maternity and Child Health Hospital.

Definition of flap necrosis

In this study, flap necrosis was diagnosed based on the observation of the flap during dressing changes within 90 days post-surgery. Epidermal Necrosis: Characterized by erythema, swelling, a glossy appearance, detachment of the epidermal layer from the dermal layer, and the presence of exudates or vesicle formation; Full-Thickness Necrosis: Identified by pallor of

the flap, diminished elasticity, darkened necrotic area, and a distinct demarcation from the surrounding normal skin.

Inclusion and exclusion criteria

Inclusion criteria: Patients definitively diagnosed with BC who underwent MRM; Patients aged 18 years or older; Patients with complete surgical and postoperative follow-up data; and Patients meeting the diagnostic criteria for flap necrosis.

Exclusion criteria: Male patients with BC; Patients whose surgery was halted intraoperatively due to other diseases; Patients with concurrent other malignant tumors; Patients with a postoperative follow-up duration of less than 90 days or with missing data exceeding 10% of key variables; Patients who had received neoadjuvant treatment (e.g., chemotherapy or radiotherapy) prior to surgery; Patients with coagulation disorders.

Study sample size and grouping

A total of 605 patients were included in this research. They were randomly allocated into a validation group (n=199) and a training group (n=406) in a 33:67 ratio. The grouping process was conducted as follows: baseline data were loaded, and categorical variables (e.g., menopausal state, history of diabetes mellitus) were transformed into factor variables, while continuous variables were designated as numeric variables. Subsequent to random sampling and grouping via the sample function, statistical tests were employed to validate the equilibrium of the grouping. For continuous variables, a normality test was performed, followed by either the t-test or Wilcoxon rank-sum test based on the results. For categorical variables, the chi-square test was applied to assess distributional differences between groups. If any variable had a *P*-value ≤0.05, the grouping was considered unbalanced, and the random grouping process was repeated until no statistically significant differences were observed for all variables (P>0.05). The final grouping was determined and saved as an Excel file, with the training group and the validation group stored in separate worksheets. This balanced grouping provided a robust foundation for subsequent model construction and validation. The detailed inclusion processes are illustrated in **Figure 1**.

Clinical data collection

Patient data were retrieved from the hospital's electronic medical record system and postoperative follow-up documentation, including preoperative, intraoperative, and postoperative information. The collected variables were categorized into clinical baseline data and laboratory data. The clinical baseline data encompassed age, body mass index (BMI), menopausal status, hypertension, diabetes, surgical duration, intraoperative bleeding volume, type of surgical incision, postoperative drainage duration, and drainage volume on postoperative day 3. The laboratory data included hemoglobin (Hb), neutrophil count (NEU), white blood cell count (WBC), platelet count (PLT), prothrombin time (PT), and fibrinogen (FIB). The primary outcome was the presence or absence of flap necrosis. During the data management process, two investigators independently verified data entry to ensure completeness and accuracy. Missing values were handled using multi-imputation technique. If the proportion of missing values exceeded 10%, the corresponding samples were excluded. Finally, all variables were meticulously screened and subsequently utilized for model construction and analysis. Note: All laboratory parameters were obtained from patients prior to the surgical procedure.

Outcome measures

Primary outcome measures: Independent risk factors were identified via multivariate Logistic regression analysis, and a Nomogram model for predicting the risk of flap necrosis following MRM was developed. The model's performance was assessed using receiver operating characteristic (ROC) curves and calibration curves in both the training and validation cohorts.

Secondary outcome measures: The baseline characteristics, including clinical baseline and laboratory data, were compared between the training and validation groups, as well as the patients with and without flap necrosis in the training set.

Statistical analyses

This research utilized SPSS 26.0 and R 4.3.3 software for data analysis and graph plotting.

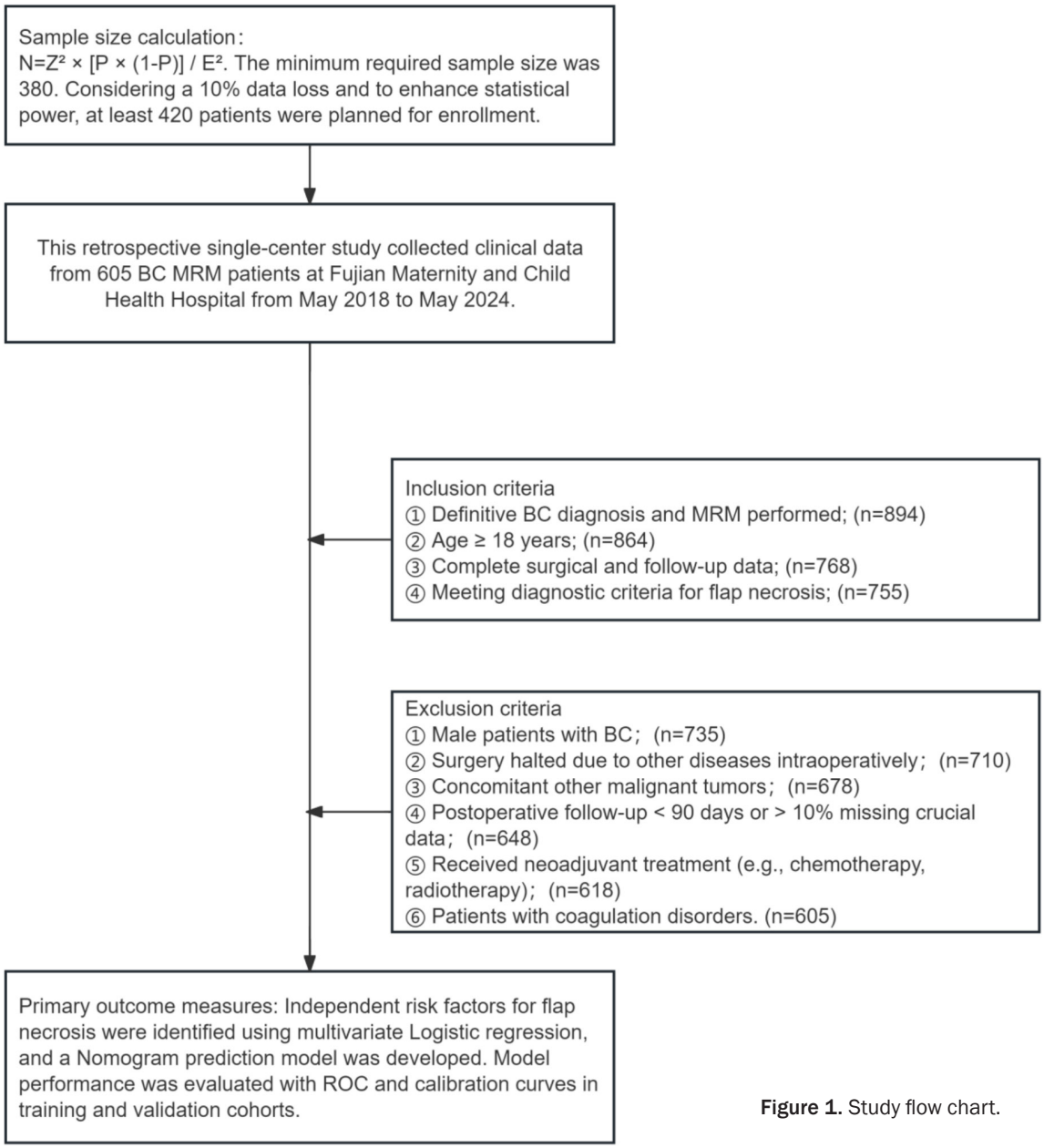

Figure 1. Study flow chart.

Categorical data were presented as frequencies and were compared between groups using the chi-square test. Continuous data were presented and compared differently depending on the distribution characteristics. Those with a normal distribution were expressed as mean ± standard deviation and analyzed using the t-test. Conversely, non-normally distributed continuous data were described as the interquartile range and analyzed using the Mann-Whitney U test. In the correlation analysis, continuous variables were transformed into binary variables based on their cut-off values, and the Spearman rank correlation test was then employed to evaluate correlations among variables. Following screening independent risk factors based on Logistic regression, a Nomogram model was established. The model's discriminatory capacity was evaluated through the ROC curve and precision-recall (PR) curve, the goodness-of-fit between the predicted and actual values was verified by the calibration curve, and the clinical utility of the model was assessed by the decision curve analysis (DCA).

All graphs were plotted using R software, with the main packages employed being pROC (for ROC curve) [15], rms (for Nomogram and calibration curve) [16], ggplot2 [17] (for data visualization), and rmda (for DCA analysis) [18].

Results

Comparison of baseline data between training and validation groups

The baseline data of patients in the training group (n=406) and the validation group (n=199) were compared, including both categorical and continuous data. Results showed that there were no statistical differences between the two groups in terms of categorical variables (e.g., the occurrence of flap necrosis, menopausal status, hypertension, diabetes, ALNM, molecular subtyping) or the continuous variables (e.g., age, BMI, WBC, Hb, PT, drainage volume on postoperative day 3) (all P>0.05, **Table 1**). The baseline characteristics of the training group and the validation group were well-balanced and comparable, ensuring the reliability of subsequent model development and validation.

Comparison of baseline data between necrosis group and non-necrosis group in the training cohort

In the training cohort, a comparative analysis was conducted on the baseline data between the necrosis group (n=94) and the non-necrosis group (n=312). In terms of categorical data, notable discrepancies were identified between groups in menopausal status (P=0.027), hypertension (P=0.044), diabetes (P=0.012), ALNM (P=0.001), transverse incision (P=0.046), surgical duration >2 hours (P<0.001), intraoperative bleeding volume ≥200 (P=0.012), and drainage duration >7 days (P=0.001). For continuous data, significant differences between the two groups were observed in age (P<0.001), BMI (P<0.001), NEU (P=0.048), Hb (P=0.049), PT (P=0.002), and drainage volume on postoperative day 3 (P=0.003). Other variables such as vascular invasion, molecular subtyping, maximum tumor diameter, and incision length did not exhibit statistically significant differences (P>0.05, **Table 2**).

Correlation analysis of differential variables

Ensure the suitability of the data for Logistic regression analysis, which is appropriate for binary outcomes, categorical variables showing significant differences were transformed into binary variables based on their cut-off values (**Table 3**). A correlation analysis was then conducted to confirm the absence of significant multicollinearity among the independent variables. The results revealed no significant linear correlation among the variables (P>0.05). The strongest negative correlation was between ALNM and surgical duration <2 hours (r=-0.126), and the strongest positive correlation was between age and BMI (r=0.138) (**Figure 2**). These results imply that the variables can be utilized as independent factors in the subsequent Logistic regression analysis.

Multivariate Logistic regression for screening independent risk factors associated with flap necrosis

Logistic regression analysis demonstrated that age (P<0.001, odds ratio [OR] =15.606, 95% confidence interval [CI]: 7.561-32.211), BMI (P=0.002, OR=2.815, 95% CI: 1.475-5.372), NEU (P=0.017, OR=0.389, 95% CI: 0.179-0.846), Hb (P<0.001, OR=0.162, 95% CI: 0.066-0.397), drainage volume on postoperative day 3 (P=0.014, OR=2.378, 95% CI: 1.190-4.754), ALNM (P=0.001, OR=0.322, 95% CI: 0.164-0.634), surgical duration >2 hours (P<0.001, OR=0.249, 95% CI: 0.123-0.504), intraoperative bleeding volume ≥200 ml (P=0.028, OR=0.457, 95% CI: 0.228-0.918), and drainage duration >7 days (P=0.010, OR=0.413, 95% CI: 0.210-0.812) were independent risk factors for flap necrosis (**Figure 3**).

Construction of the Nomogram prediction model

Based on the results of the multivariate Logistic regression analysis, nine significant factors including age, BMI, NEUT, Hb, drainage volume on postoperative day 3, ALNM, surgical duration, intraoperative bleeding volume, and drainage duration were identified. A Nomogram prediction model was constructed to visually represent the contribution of each variable to the risk of flap necrosis (**Figure 4**). The model assigns scaled line segments to each variable, allowing for an intuitive calculation of the total risk score. In addition, a model formula was derived based on the regression coefficients of the aforementioned variables: Logit(p) = -1.245 + 2.708 × (Age ≥55.5) + 1.200 × (BMI

Table 1. Comparison of baseline data between training group and validation group

Counting data	Total	Validation group (n=199)	Training group (n=406)	Statistic	P
Flap necrosis					
With	133	39	94	0.984	0.321
Without	472	160	312		
Pausimenia					
Yes	342	116	226	0.375	0.540
No	263	83	180		
Hypertension					
With	87	26	61	0.416	0.519
Without	518	173	345		
Diabetes					
With	69	21	48	0.213	0.644
Without	536	178	358		
Axillary lymph node metastasis					
With	270	92	178	0.308	0.579
Without	335	107	228		
Vascular invasion					
With	33	8	25	1.183	0.277
Without	572	191	381		
Clinical staging					
I	116	43	73	1.714	0.424
II	319	98	221		
III	170	58	112		
Molecular subtyping					
Luminal A	87	27	60	1.061	0.900
Luminal B (HER-2 negative)	216	69	147		
Luminal B (HER-2 positive)	99	33	66		
HER-2 overexpression	62	19	43		
Triple-negative	141	51	90		
Transverse incision					
Yes	363	124	239	0.660	0.416
No	242	75	167		
Surgical duration >2 hours					
Yes	342	117	225	0.619	0.431
No	263	82	181		
Intraoperative bleeding volume ≥200 ml					
Yes	170	52	118	0.569	0.451
No	435	147	288		
Drainage duration >7 days					
Yes	337	107	230	0.449	0.503
No	268	92	176		
Age (years)	53.036±7.252	52.698±7.418	53.202±7.174	0.802	0.423
BMI (kg/m^2)	24.263±3.442	24.137±3.299	24.325±3.512	0.633	0.527
WBC (×10^9/L)	5.96 [3.92, 7.77]	5.52 [4.06, 7.60]	6.05 [3.86, 7.90]	0.523	0.601
NEU (×10^9/L)	61.402±14.807	61.462±14.132	61.372±15.143	-0.070	0.944
Hb (g/L)	126.972±25.725	126.548±25.369	127.180±25.927	0.284	0.777
PLT (×10^9/L)	232.263±48.827	230.231±50.641	233.259±47.945	0.716	0.474
PT (seconds)	12.00 [10.00, 14.00]	12.00 [10.00, 14.00]	12.00 [10.00, 13.00]	0.650	0.516
APTT (seconds)	28.547±8.790	28.447±8.469	28.596±8.953	0.195	0.845
FIB (g/L)	292.412±41.348	292.523±43.006	292.357±40.565	-0.046	0.963
Maximum tumor diameter (cm)	4.75 [3.14, 6.33]	4.47 [2.79, 6.38]	4.81 [3.21, 6.28]	0.609	0.542
Incision length (cm)	16.256±5.121	16.293±4.998	16.238±5.187	-0.125	0.901
Drainage volume on postoperative day 3 (mL)	227.190±45.251	228.155±44.813	226.718±45.511	-0.367	0.714

Note: HER-2, human epidermal growth factor receptor 2; BMI, body mass index; WBC, white blood cell count; NEU, neutrophil count; Hb, hemoglobin; PLT, platelet count; PT, prothrombin time; APTT, activated partial thromboplastin time; FIB, fibrinogen.

Table 2. Comparison of baseline data between patients with and without flap necrosis in the training cohort

Categorical data	Total	Necrosis group (n=94)	Non-necrosis group (n=312)	Statistic	P
Pausimenia					
Yes	226	43	183	4.878	0.027
No	180	51	129		
Hypertension					
With	61	8	53	4.065	0.044
Without	345	86	259		
Diabetes					
With	48	18	30	6.298	0.012
Without	358	76	282		
Axillary lymph node metastasis					
With	178	55	123	10.689	0.001
Without	228	39	189		
Vascular invasion					
With	25	7	18	0.352	0.553
Without	381	87	294		
Clinical staging					
I	73	15	58	2.686	0.261
II	221	58	163		
III	112	21	91		
Molecular subtyping					
Luminal A	60	11	49	2.840	0.585
Luminal B (HER-2 negative)	147	37	110		
Luminal B (HER-2 positive)	66	15	51		
HER-2 overexpression	43	13	30		
Triple-negative	90	18	72		
Transverse incision					
Yes	239	47	192	3.972	0.046
No	167	47	120		
Surgical duration >2 hours					
Yes	225	68	157	14.177	<0.001
No	181	26	155		
Intraoperative bleeding volume ≥200 ml					
Yes	118	37	81	6.291	0.012
No	288	57	231		
Drainage duration >7 days					
Yes	230	67	163	10.656	0.001
No	176	27	149		
Age (years)	53.202±7.174	59.426±6.272	51.327±6.326	-10.902	<0.001
BMI (kg/m^2)	24.325±3.512	26.046±3.718	23.807±3.281	-5.618	<0.001
WBC (×10^9/L)	6.05 [3.86, 7.90]	5.85 [3.66, 7.95]	6.08 [3.89, 7.77]	0.305	0.760
NEU (×10^9/L)	61.372±15.143	58.664±13.079	62.188±15.639	1.985	0.048
Hb (g/L)	127.180±25.927	122.564±30.771	128.571±24.163	1.976	0.049
PLT (×10^9/L)	233.00 [201.25, 261.50]	223.50 [201.00, 251.25]	234.50 [202.00, 265.00]	1.927	0.054
PT (seconds)	12.00 [10.00, 13.00]	12.50 [10.00, 14.75]	11.00 [10.00, 13.00]	3.087	0.002
APTT (seconds)	28.596±8.953	29.957±8.633	28.186±9.020	-1.686	0.093
FIB (g/L)	292.357±40.565	289.540±38.292	293.206±41.247	0.768	0.443
Maximum tumor diameter (cm)	4.81 [3.21, 6.28]	4.62 [3.63, 5.55]	4.88 [3.14, 6.50]	1.029	0.304
Incision length (cm)	16.238±5.187	16.737±5.162	16.087±5.193	-1.065	0.288
Drainage volume on postoperative day 3	226.718±45.511	239.036±47.200	223.006±44.400	-3.024	0.003

Note: HER-2, human epidermal growth factor receptor 2; BMI, body mass index; WBC, white blood cell count; NEU, neutrophil count; Hb, hemoglobin; PLT, platelet count; PT, prothrombin time; APTT, activated partial thromboplastin time; FIB, fibrinogen.

Table 3. Assignments of differential variables

Variable name	Variable attribute	Assignment content
Flap necrosis	(Y)	Yes = 1, no = 2
Age	(X)	It belongs to a continuous variable and is classified using the cut-off value (<55.5 = 2, ≥55.5 = 1)
BMI	(X)	It belongs to a continuous variable and is classified using the cut-off value (<25.53 = 2, ≥25.53 = 1)
NEU	(X)	It belongs to a continuous variable and is classified using the cut-off value (<70.8 = 2, ≥70.8 = 1)
Hb	(X)	It belongs to a continuous variable and is classified using the cut-off value (<96.5 = 2, ≥96.5 = 1)
PT	(X)	It belongs to a continuous variable and is classified using the cut-off value (<11.5 = 2, ≥11.5 = 1)
Drainage volume on postoperative day 3	(X)	It belongs to a continuous variable and is classified using the cut-off value (<254.225 = 2, ≥254.225 = 1)
Pausimenia	(X)	Yes = 1, no = 2
Hypertension	(X)	With = 1, without = 2
Diabetes	(X)	With = 1, without = 2
Axillary lymph node metastasis	(X)	With = 1, without = 2
Transverse incision	(X)	Yes = 1, no = 2
Surgical duration <2 h	(X)	Yes = 1, no = 2
Intraoperative bleeding volume <200 ml	(X)	Yes = 1, no = 2
Drainage duration <7 days	(X)	Yes = 1, no = 2

Note: Y: dependent variable, X: independent variable. BMI, body mass index; WBC, white blood cell count; NEU, neutrophil count; Hb, hemoglobin; PLT, platelet count; PT, prothrombin time; APTT, activated partial thromboplastin time; FIB, fibrinogen.

≥25.53) - 0.974 × (NEU≥70.8) - 1.883 × (Hb≥96.5) + 0.983 × (Drainage Volume on Postoperative Day 3 ≥254.225) - 1.093 × (Axillary Lymph Node Metastasis Yes) + 1.441 × (Surgery Duration No) + 0.740 × (Intraoperative Bleeding Volume No) + 0.914 × (Drainage Duration No). The total score calculated from the Nomogram is mapped to the predicted risk axis, providing a quantitative assessment of the risk of postoperative flap necrosis.

Internal validation results of model performance and predictive capability assessment

In the training group, the risk score of each patient was computed and a grouped comparison was carried out based on the flap necrosis status. A significant difference in risk scores was observed between the two groups (P< 0.001, **Figure 5A**). The ROC curve of the model manifested its outstanding discriminatory power, with an AUC value of 0.898 (95% CI: 0.861-0.934). The PR curve further confirmed the model's accuracy and sensitivity in classification tasks (**Figure 5B**, **5C**). The calibration curve indicated good agreement between predicted probabilities and the actual outcomes. The chi-square value of the goodness-of-fit test was 11.478 (P=0.1761), suggesting that the model possessed a sound calibration ability (**Figure 5D**). The DCA demonstrated that the model yielded clinical benefits within a risk threshold range of 0-98%, with a maximum benefit rate of 76.84% (**Figure 5E**). The likelihood ratio test yielded a chi-square value of 178.68 (P<0.001), confirming the statistical significance of the model. Collectively, the model demonstrated excellent performance in terms of discrimination, calibration, and clinical applicability in the training group, indicating its high predictive value for postoperative flap necrosis risk.

Performance evaluation of the Nomogram prediction model in the validation group

In the validation cohort, significant differences in risk scores were observed between patients with and without flap necrosis (P<0.001, **Figure 6A**). The model demonstrated strong discrimi-

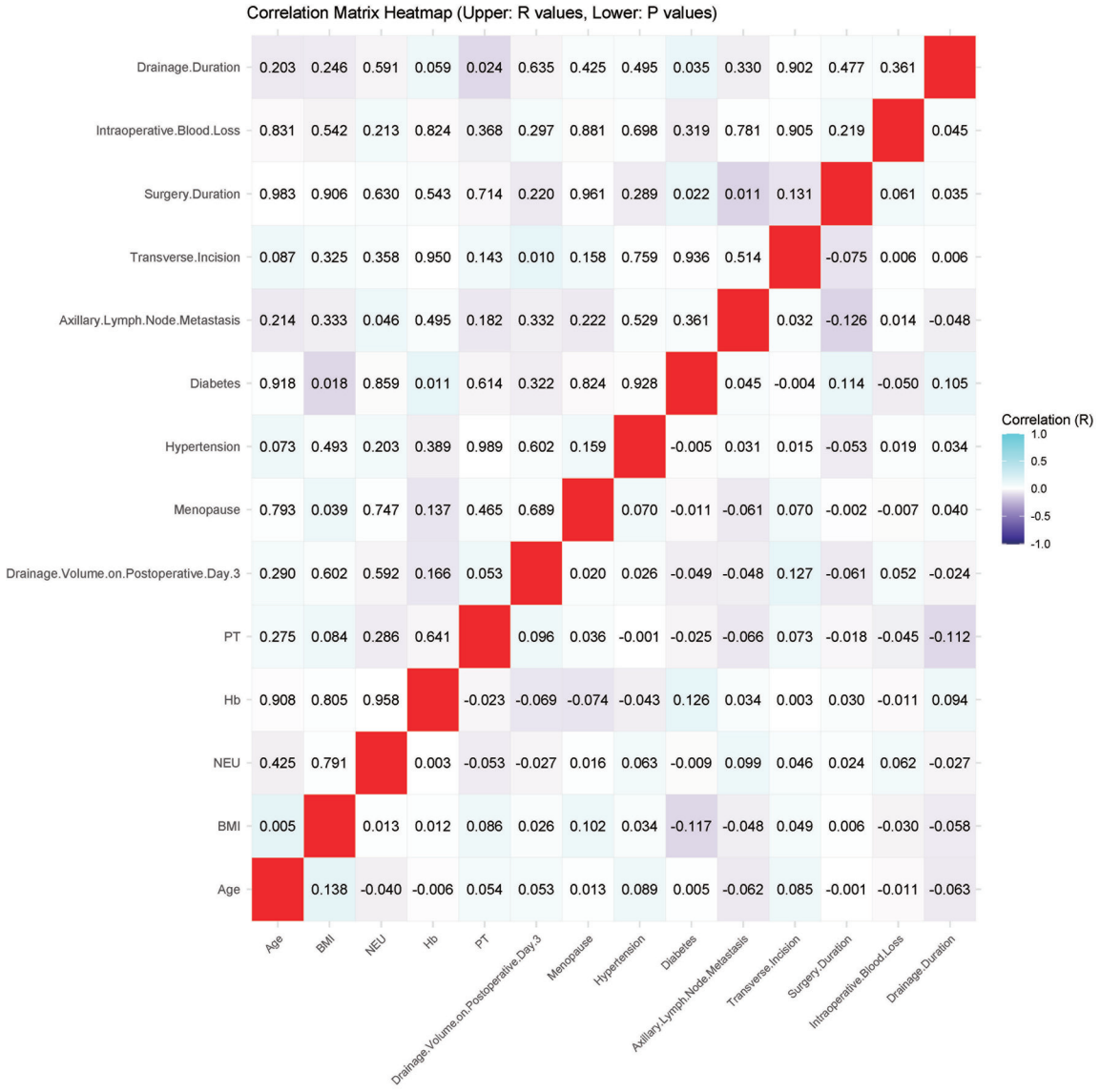

Figure 2. Correlation analysis matrix of differential variables.

nation, with an AUC of 0.886 (95% CI: 0.825-0.948), highlighting its robust predictive capacity (**Figure 6B**). The PR curve further validated the model's accuracy and sensitivity in classification tasks (**Figure 6C**). The calibration curve indicated excellent agreement between predicted probabilities and actual outcomes, supported by the goodness-of-fit test (χ^2=4.3268, P=0.8265, **Figure 6D**). The DCA demonstrated clinical utility across a threshold probability range of 0-97%, with a maximum net benefit rate of 80.40% (**Figure 6E**). Additionally, the likelihood ratio test confirmed the statistical significance of the model, with a chi-square value of 78.723 (P<0.001). Overall, the model exhibited excellent performance in terms of discrimination, calibration, and clinical applicability, providing reliable predictions for the validation group. DeLong's test for two ROC curves showed no significant difference in AUCs between the training and validation groups (0.898 vs. 0.886; D=0.309, df=341.430, P=0.756), indicating comparable performance in the two sets. Overall, the model exhibited excellent performance in terms of discrimination, calibration, and clinical applicability, providing reliable predictions for the validation group.

Characteristics	β	OR value	HR (95% CI)	P value
Age	2.748	15.606	15.606(7.561-32.211)	<0.001
BMI	1.035	2.815	2.815(1.475-5.372)	0.002
NEU	-0.945	0.389	0.389(0.179-0.846)	0.017
Hb	-1.821	0.162	0.162(0.066-0.397)	<0.001
PT	0.413	1.512	1.512(0.793-2.882)	0.210
Drainage Volume on Postoperative Day 3	0.866	2.378	2.378(1.190-4.754)	0.014
Menopause	0.502	1.651	1.651(0.869-3.140)	0.126
Hypertension	0.600	1.822	1.822(0.616-5.389)	0.278
Diabetes mellitus	-0.335	0.715	0.715(0.275-1.862)	0.492
Axillary lymph node metastasis	-1.132	0.322	0.322(0.164-0.634)	0.001
Transverse incision	0.323	1.381	1.381(0.720-2.650)	0.331
Surgical time < 2h	-1.391	0.249	0.249(0.123-0.504)	<0.001
Intraoperative bleeding <200ml	-0.782	0.457	0.457(0.228-0.918)	0.028
Drainage time <7d	-0.885	0.413	0.413(0.210-0.812)	0.010

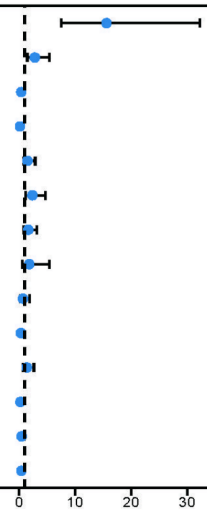

Figure 3. Logistic regression for screening independent risk factors associated with flap necrosis. Note: BMI, body mass index; WBC, white blood cell count; NEU, neutrophil count; Hb, hemoglobin; PLT, platelet count; PT, prothrombin time; APTT, activated partial thromboplastin time; FIB, fibrinogen.

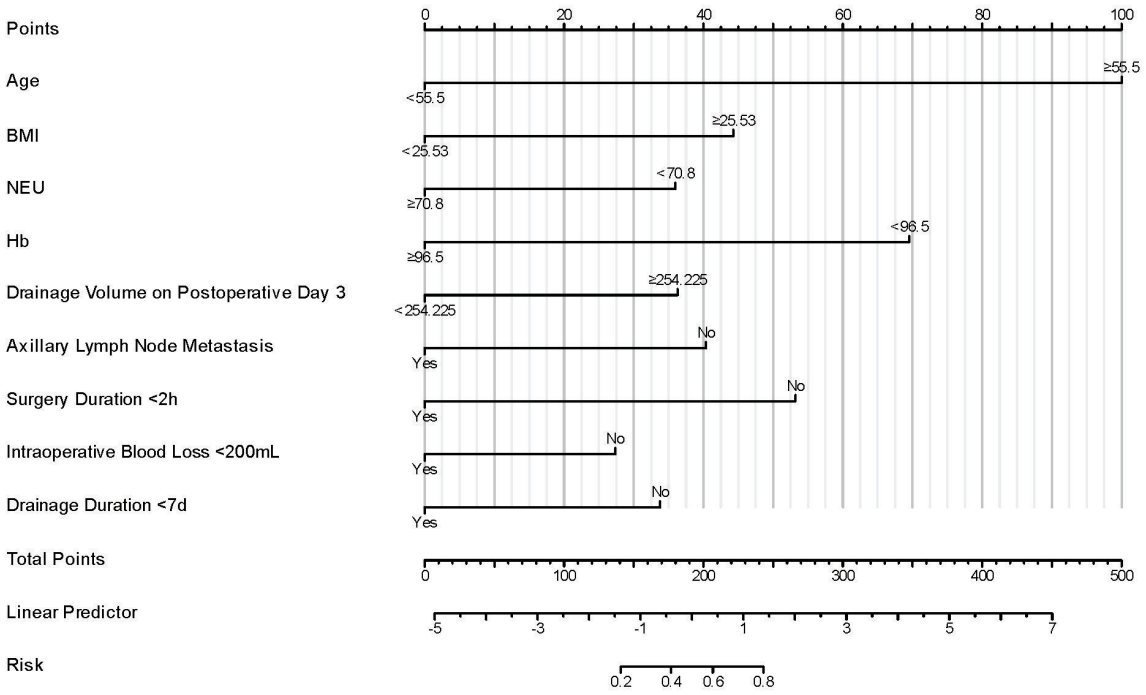

Figure 4. Construction of the Nomogram model.

Display of model performance indicators

The Risk 1 (training group) model performed well in the training group, with a specificity of 87.50%, a sensitivity of 77.66%, a Youden index of 65.16%, a cut-off value of 0.777, an accuracy of 85.22%, a precision of 77.66%, and an F1 value of 89.18%. The Risk 2 (validation group) model also had relatively good performance in the validation group, with a specificity of 81.88%, a sensitivity of 82.05%, a Youden index of 63.93%, a cut-off value of 1.174, an accuracy of 81.91%, a precision of 82.05%, and an F1 value of 92.09%. These

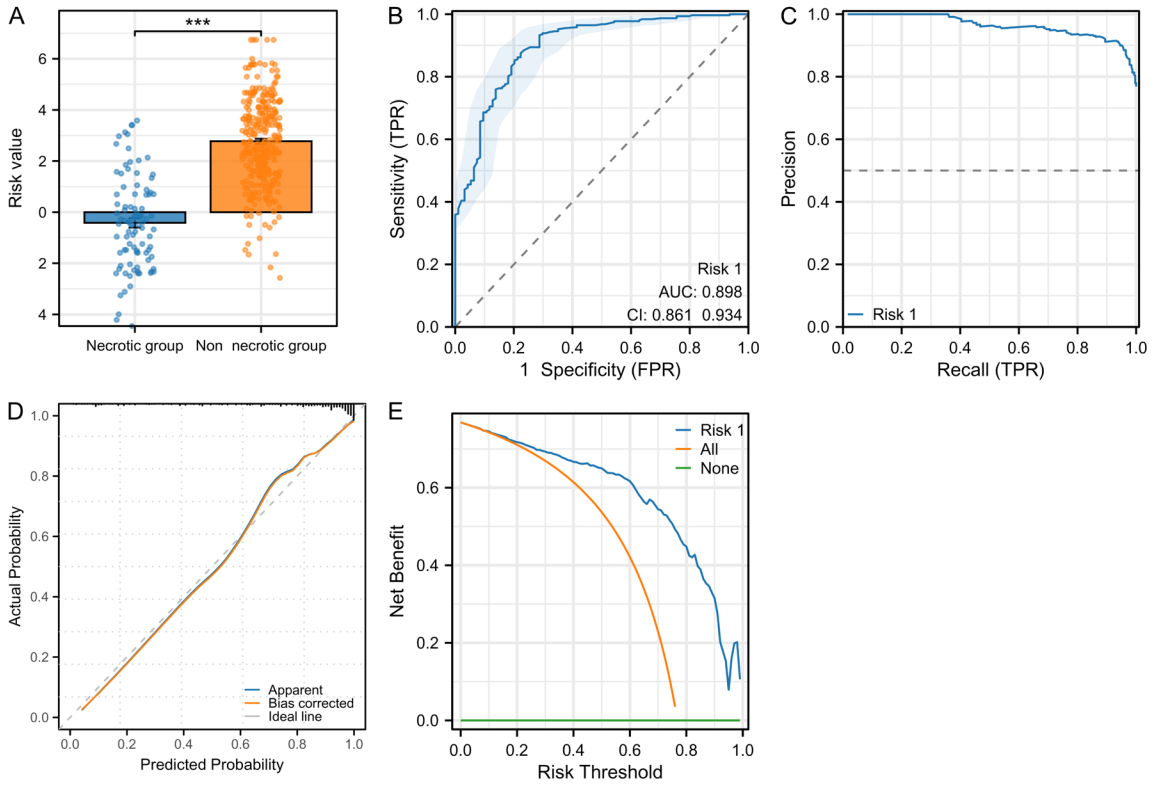

Figure 5. Model prediction in the training group. A: Comparison of risk score between patients with and without flap necrosis in the training group. B: Receiver operating characteristic (ROC) curve of the prediction model in the training group. C: Precision-recall (PR) curve of the prediction model in the training group. D: Calibration curve of the prediction model in the training group. E: Decision curve of the prediction model in the training group.

results indicate that the model has certain predictive value in both the training group and the validation group. See **Table 4**.

Discussion

By utilizing large-sample clinical data from patients who underwent modified radical mastectomy (MRM) for BC, this study developed a risk prediction model for flap necrosis using Logistic regression analysis. The model was visualized through a Nomogram, demonstrating potential applicability in risk evaluation. The investigation identified age, BMI, NEU, Hb, drainage volume on postoperative day 3, ALNM, surgical duration, intraoperative bleeding volume, and drainage duration as independent risk factors for flap necrosis. The model exhibited high discriminatory power and calibration accuracy in both the training and validation cohorts, underscoring its practical value in predicting postoperative flap necrosis risk. These findings not only provide clinicians with distinct high-risk factors but also present a scientific foundation for individualized risk assessment and precise intervention, ultimately enhancing patient prognosis and reducing the incidence of flap necrosis.

Elderly patients often experience a declined tissue repair capacity and diminished vascular elasticity, resulting in insufficient blood supply following surgery and restricted flap healing [19]. Higher BMI is associated with a thicker subcutaneous fat layer, which increases the risk of local ischemic injury, incision tension, and infection [20]. Evidence suggests that BMI is a significant independent risk factor for various surgical complications, particularly flap necrosis after BC surgery [21]. Additionally, Hassan et al. [22] employed machine learning analysis and indicated that BMI and age are crucial predictors of flap necrosis, which aligns with the results of this present study. These findings collectively substantiate the necessity of preoperative intervention for elderly or obese patients, including optimizing nutrition and postoperative care strategies.

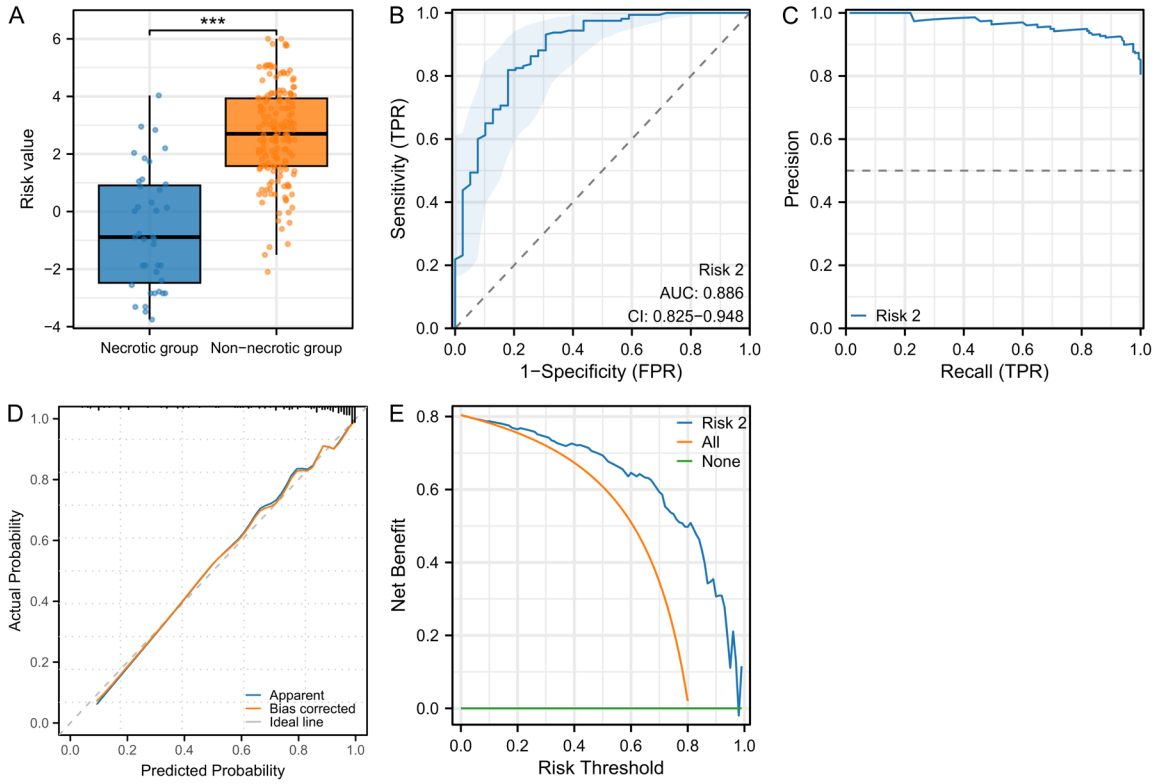

Figure 6. Model prediction in the validation group. A: Comparison of risk score between patients with and without flap necrosis in the validation group. B: Receiver operating characteristic (ROC) curve of the prediction model in the validation group. C: Precision-recall (PR) curve of the prediction model in the validation group. D: Calibration curve of the prediction model in the validation group. E: Decision curve of the prediction model in the validation group.

Table 4. Predictive performance of the model for flap necrosis in patients of two sets

	Specificity	Sensitivity	Youden index	Cut off	Accuracy	Precision	F1 Score
Risk 1	87.50%	77.66%	65.16%	0.777	85.22%	77.66%	89.18%
Risk 2	81.88%	82.05%	63.93%	1.174	81.91%	82.05%	92.09%

Note: Risk 1: training set; Risk 2: validation set.

Elevated neutrophil counts and lower hemoglobin levels are tightly linked to flap necrosis. In this study, a diminished proportion of NEU (<70.8%) may indicate a compromised postoperative immune response, which impedes wound healing. Besides, an Hb level beneath 96.5 g/L suggests insufficient systemic oxygen supply, which aggravates local ischemia and hypoxia. Rahimi et al. [23] demonstrated that preoperative optimization of Hb levels improves flap survival rates and reduces postoperative complications. Moreover, Shi et al. [24] further corroborated the reliability of Hb as a risk indicator for postoperative complications, particularly in microvascular free flap transplantation.

A drainage volume ≥254.225 mL on the third postoperative day and a drainage duration exceeding 7 days were markedly correlated with a heightened risk of flap necrosis. Excessive drainage may indicate a heightened local exudative response, potentially signaling infection or poor wound healing. Ouyang et al. [25] noted that the increase in postoperative exudation is intimately linked to wound infection and disrupted blood supply, which aligns with our observations. Additionally, Lu et al. [26] illustrated that excessive exudate not only delays healing but also increases the risk of flap necrosis.

ALNM, surgical duration exceeding 2 hours, and intraoperative bleeding volume ≥200 mL were also identified as crucial risk factors for flap necrosis. Moo et al. [27] found that prolonged surgical duration and substantial intraoperative blood loss remarkably elevated the

risk of flap necrosis. Additionally, Liu et al. [24] emphasized the importance of intraoperative vascular protection and fluid management in reducing flap necrosis risk. The results of this study are highly consistent with these findings, suggesting that optimizing intraoperative procedures and shortening surgical duration may effectively enhance postoperative prognosis.

In this study, diabetes was found to be associated with flap necrosis but was not recognized as an independent prognostic factor in the multivariate analysis. This suggests that diabetes may indirectly hinder wound healing by impairing patient's local blood circulation and immune function, rather than acting as a direct causative factor. Nevertheless, the potential role of diabetes in flap healing cannot be overlooked. Lu et al. [26] discovered that preoperative infection is a significant contributor to postoperative necrosis in soft tissue defect repair. This highlights the potential synergistic effect of diabetes and infection in increasing the risk of flap necrosis. Therefore, preoperative optimization glycemic control and infection prevention are critical strategies for reducing the risk of flap necrosis.

The developed prediction model in this study showed high performance in both the training group and the validation group. In the training cohort, the model demonstrated an AUC value of 0.898 (95% CI: 0.861-0.934), a specificity of 87.50%, and a sensitivity of 77.66%, exemplifying its remarkable discriminatory capacity. In the validation cohort, the model had an AUC value of 0.886 (95% CI: 0.825-0.948), with specificity and sensitivity of 81.88% and 82.05%, respectively, maintaining its stability and generalizability during external validation. In addition, the DCA revealed that the model conferred a relatively high clinical benefit within the risk threshold range spanning from 0 to 97%, with a maximum benefit rate reaching 76.84% and 80.40% in the training and validation groups, further corroborating the model's applicability in clinical practice. In the study by Yang et al. [28], the machine learning model achieved an AUC of 0.828 in predicting vascular complications after free flap reconstruction, which emphasized the potential of integrating multi-dimensional factors to enhance prediction performance in complex models. This echoes the comprehensive inclusion of perioperative factors in our model, further substantiating the superiority of multi-dimensional analysis. Similarly, in the study by Wang et al. [29], the XGBoost model was employed to prognosticate the reoperation rate and readmission rate 30 days after head and neck free flap surgery, obtaining AUC values of 0.78 and 0.58, respectively, demonstrating the application potential of machine learning in predicting postoperative complications. The random forest model has also been applied in predicting breast flap necrosis. As shown in the study by Hassan et al. [22], it had an AUC value of 0.70, with a significant net benefit within a specific probability threshold range as indicated by DCA. These results are consistent with the findings of DCA in the present study, further accentuating the clinical utility of the prediction model. Furthermore, in the study by Tarle et al. [30], the HALP score was employed to assess the risk of complications following head and neck free flap reconstruction, attaining an AUC value as high as 0.85. Their study underscored the significance of multi-dimensional indices from the perspective of immunity and nutrition, which aligns with the concept of integrated analysis of perioperative indicators in our study. Moreover, the study by Hansen et al. [31] revealed that the Extended Breast Reconstruction Risk Assessment Score could predict the incidence of breast flap necrosis and was notably correlated with relevant risk factors such as advanced age, smoking, and postoperative infection. This is highly congruent with the risk factors like high BMI and age identified in our study, further supporting the scientific validity of our model.

Although this study offers a valuable instrument for the risk evaluation of flap necrosis, it is not without limitations. First, this is a single-center retrospective study where all the data were sourced from a single medical institution. This may introduce sample selection bias and constrain the generalizability of the model. Although the model demonstrated satisfactory performance in internal validation, its stability and external applicability require further assessment through multi-center, large-sample external validation. Second, the retrospective collection of data might have overlooked some crucial variables, such as intraoperative hemodynamic alterations, the circumstances of postoperative antibiotic administration, and other dynamic factors that could potentially have an

interfering effect on the prediction results. Third, this study did not comprehensively account for the potential influence of postoperative adjuvant therapies, like radiotherapy and chemotherapy, on flap healing. This limitation may restrict the model's capacity to reflect long-term postoperative recovery.

To further enhance the prediction model of this study, future research endeavors could be initiated from the following perspectives. First, it is essential to expand the sample size and integrate data from a greater number of medical institutions. By means of multi-center collaboration, the applicability of the model can be meticulously verified, thereby mitigating the influence of single-center data bias on the research findings. Second, postoperative treatment and follow-up data could be incorporated to formulate a dynamic prediction model. This would enable a more comprehensive and in-depth assessment of patients' postoperative recovery. Third, the exploration of other machine learning algorithms, such as random forest and XGBoost, should be actively pursued. This would serve to optimize the modeling strategy and elevate the prediction precision of the model. Fourth, in conjunction with molecular biological markers, including genomics and metabolomics data, an in-depth exploration into the underlying molecular mechanisms of flap necrosis could be carried out. These efforts will ultimately contribute to improved risk management and patient outcomes in breast cancer surgery.

Conclusion

The risk prediction model developed in this study, based on perioperative indicators, demonstrated excellent discrimination, calibration, and clinical applicability in both the training group and the validation group. By quantifying key risk factors, such as age, BMI, neutrophil count, hemoglobin levels, drainage volume, and surgical duration, the model provides a reliable tool for assessing the risk of flap necrosis following MRM for breast cancer.

Disclosure of conflict of interest

None.

Address correspondence to: Yi Peng, Department of Breast Surgery, Fujian Maternity and Child Health Hospital, No. 18 Dao Shan Road, Gulou District, Fuzhou 350001, Fujian, China. Tel: +86-0591-87626063; E-mail: pengyi831010@163.com

References

[1] Giaquinto AN, Sung H, Newman LA, Freedman RA, Smith RA, Star J, Jemal A and Siegel RL. Breast cancer statistics 2024. CA Cancer J Clin 2024; 74: 477-495.

[2] Loibl S, Poortmans P, Morrow M, Denkert C and Curigliano G. Breast cancer. Lancet 2021; 397: 1750-1769.

[3] Sung H, Ferlay J, Siegel RL, Laversanne M, Soerjomataram I, Jemal A and Bray F. Global cancer statistics 2020: GLOBOCAN estimates of incidence and mortality worldwide for 36 cancers in 185 countries. CA Cancer J Clin 2021; 71: 209-249.

[4] Cao W, Chen HD, Yu YW, Li N and Chen WQ. Changing profiles of cancer burden worldwide and in China: a secondary analysis of the global cancer statistics 2020. Chin Med J (Engl) 2021; 134: 783-791.

[5] Loibl S, André F, Bachelot T, Barrios CH, Bergh J, Burstein HJ, Cardoso MJ, Carey LA, Dawood S, Del Mastro L, Denkert C, Fallenberg EM, Francis PA, Gamal-Eldin H, Gelmon K, Geyer CE, Gnant M, Guarneri V, Gupta S, Kim SB, Krug D, Martin M, Meattini I, Morrow M, Janni W, Paluch-Shimon S, Partridge A, Poortmans P, Pusztai L, Regan MM, Sparano J, Spanic T, Swain S, Tjulandin S, Toi M, Trapani D, Tutt A, Xu B, Curigliano G and Harbeck N; ESMO Guidelines Committee. Electronic address: clinicalguidelines@esmo.org. Early breast cancer: ESMO clinical practice guideline for diagnosis, treatment and follow-up. Ann Oncol 2024; 35: 159-182.

[6] Chen JC, Li Y, Fisher JL, Bhattacharyya O, Tsung A, Bazan JG and Obeng-Gyasi S. Modified radical mastectomy in de novo stage IV inflammatory breast cancer. Ann Surg Oncol 2022; 29: 6681-6688.

[7] Dong B, Yin X, Xu H, Zhou K, Li L, Tian B and Cui R. Application value of modified radical mastectomy in female patients with breast cancer of different molecular types: a prognosis study. Am J Transl Res 2022; 14: 2490-2496.

[8] Ishibashi N, Nishimaki H, Maebayashi T, Adachi K, Sakurai K, Masuda S, Hata M and Okada M. Partial chest wall radiation therapy for positive or close surgical margins after modified radical mastectomy for breast cancer without lymph node metastasis. Asia Pac J Clin Oncol 2020; 16: 28-33.

[9] Jia H, Bai W, Li Z and Li Y. Comparative study of efficacy of breast-conserving surgery and

modified radical mastectomy in treating early breast cancer. Panminerva Med 2023; 65: 102-103.
[10] Musavi L, Bingham EG, Anderson L, Alnaseri T, Demirjian M, Kwan L, Crisera C, Festekjian J and DeLong MR. Impact of mastectomy flap necrosis on prepectoral reconstructive outcomes. J Plast Reconstr Aesthet Surg 2024; 91: 128-134.
[11] Ray HR, Doren EL, Adamson K, Kong AL and Cortina CS. Risk factors for skin flap and nipple-areolar necrosis in patients undergoing nipple-sparing mastectomy with deep inferior epigastric perforator flap reconstruction. Am Surg 2024; 90: 2769-2779.
[12] Qiu X, Sun X and Huang G. Immediate flap increases patient safety for deep sternal wound infection: a meta-analysis. Int Wound J 2023; 20: 3271-3278.
[13] Gold HT, Do HT and Dick AW. Correlates and effect of suboptimal radiotherapy in women with ductal carcinoma in situ or early invasive breast cancer. Cancer 2008; 113: 3108-3115.
[14] Pagliara D, Schiavone L, Garganese G, Bove S, Montella RA, Costantini M, Rinaldi PM, Bottosso S, Grieco F, Rubino C, Salgarello M and Ribuffo D. Predicting mastectomy skin flap necrosis: a systematic review of preoperative and intraoperative assessment techniques. Clin Breast Cancer 2023; 23: 249-254.
[15] Robin X, Turck N, Hainard A, Tiberti N, Lisacek F, Sanchez JC and Müller M. pROC: an open-source package for R and S+ to analyze and compare ROC curves. BMC Bioinformatics 2011; 12: 77.
[16] Li M, Wei X, Zhang SS, Li S, Chen SH, Shi SJ, Zhou SH, Sun DQ, Zhao QY and Xu Y. Recognition of refractory Mycoplasma pneumoniae pneumonia among Myocoplasma pneumoniae pneumonia in hospitalized children: development and validation of a predictive nomogram model. BMC Pulm Med 2023; 23: 383.
[17] Gustavsson EK, Zhang D, Reynolds RH, Garcia-Ruiz S and Ryten M. ggtranscript: an R package for the visualization and interpretation of transcript isoforms using ggplot2. Bioinformatics 2022; 38: 3844-3846.
[18] Liu C, He Y and Luo J. Application of chest CT imaging feature model in distinguishing squamous cell carcinoma and adenocarcinoma of the lung. Cancer Manag Res 2024; 16: 547-557.
[19] Rees A, Fishman EK, Chu LC, Rowe SP and Rizk RC. New old age meets the same old ageism: leveraging technology to promote healthier aging. J Am Coll Radiol 2024; 21: 1830-1831.
[20] Kim HB, Kim YS, Eom JS and Han HH. Analysis of flap thickness to breast projection ratio correlating to body mass index and age in East Asian women: considerations in flap selection in breast reconstruction. Microsurgery 2024; 44: e31177.
[21] Ito H, Ueno T, Suga H, Shiraishi T, Isaka H, Imi K, Miyamoto K, Tada M, Ishizaka Y and Imoto S. Risk factors for skin flap necrosis in breast cancer patients treated with mastectomy followed by immediate breast reconstruction. World J Surg 2019; 43: 846-852.
[22] Hassan AM, Biaggi AP, Asaad M, Andejani DF, Liu J, Offodile Nd AC, Selber JC and Butler CE. Development and assessment of machine learning models for individualized risk assessment of mastectomy skin flap necrosis. Ann Surg 2023; 278: e123-e130.
[23] Rahimi A, Zhang Y, Kim DW, Morgan H, Hossain F, Leitch M, Wooldridge R, Seiler S, Goudreau S, Haley B, Rao R, Rivers A, Spangler A, Ahn C, Stevenson S, Staley J, Albuquerque K, Ding C, Gu X, Zhao B and Timmerman R. Risk factors for fat necrosis after stereotactic partial breast irradiation for early-stage breast cancer in a phase 1 clinical trial. Int J Radiat Oncol Biol Phys 2020; 108: 697-706.
[24] Liu H, Liu J, Wu Y, Ma Y, Zhou M, Xue Y and Rui Y. Analysis of the risk factors for free flap necrosis in soft tissue reconstruction of the lower limbs. Orthop Surg 2023; 15: 1534-1540.
[25] Ouyang SB, Wu ZH, Zhang YP and Lu XL. Comprehensive analysis of risk factors for flap necrosis in free flap reconstruction of postoperative tissue defects in oral and maxillofacial tumors. Sci Rep 2024; 14: 18676.
[26] Lu Y, Shen D, Cao J, Huang X and Zhou J. Effects of anterolateral femoral free flap transplantation on the repair of soft tissue defect of hands and feet and risk factors for flap necrosis. Am J Transl Res 2023; 15: 3631-3638.
[27] Moo TA, Nelson JA, Sevilimedu V, Charyn J, Le TV, Allen RJ, Mehrara BJ, Barrio AV, Capko DM, Pilewskie M, Heerdt AS, Tadros AB, Gemignani ML, Morrow M and Sacchini V. Strategies to avoid mastectomy skin-flap necrosis during nipple-sparing mastectomy. Br J Surg 2023; 110: 831-838.
[28] Yang JJ, Liang Y, Wang XH, Long WY, Wei ZG, Lu LQ, Li W and Shao X. Prediction of vascular complications in free flap reconstruction with machine learning. Am J Transl Res 2024; 16: 817-828.
[29] Wang SY, Barrette LX, Ng JJ, Sangal NR, Cannady SB, Brody RM, Bur AM and Brant JA. Predicting reoperation and readmission for head and neck free flap patients using machine learning. Head Neck 2024; 46: 1999-2009.

[30] Tarle M, Čvrljević I, Raguž M and Lukšić I. Hemoglobin-albumin-lymphocyte-platelet (HALP) score as a predictive model for the success of reconstruction of head and neck defects with free microvascular flaps. J Clin Med 2023; 12: 5314.

[31] Hansen N, Espino S, Blough JT, Vu MM, Fine NA and Kim JYS. Evaluating mastectomy skin flap necrosis in the extended breast reconstruction risk assessment score for 1-year prediction of prosthetic reconstruction outcomes. J Am Coll Surg 2018; 227: 96-104.